


 Cite this: *RSC Adv.*, 2023, **13**, 33376

## Surface-modified silicalite-1-filled PDMS membranes for pervaporation dehydration of trichloroethylene

 Xiaosan Song,<sup>\*ab</sup> Xichen Song,<sup>a</sup> Bo Liu<sup>a</sup> and Zilin Yue<sup>a</sup>

In this study, the impact of silane coupling agents, namely 3-aminopropyltrimethoxysilane (APTMS), trimethylchlorosilane (TMCS), and 1,1,3,3-tetramethyldisilazane (TMDS), on the hydrophobicity of silicalite-1 zeolite was investigated to enhance the pervaporation separation performance of mixed matrix membranes (MMMs) for trichloroethylene (TCE). The hydrophobicity of TMCS@silicalite-1 and TMDS@silicalite-1 particles exhibited significant improvement, as evidenced by the increase in water contact angle from 96.1° to 101.9° and 109.1°, respectively. Conversely, the water contact angle of APTMS@silicalite-1 particles decreased to 85.2°. Silane-modified silicalite-1 particles were incorporated into polydimethylsiloxane (PDMS) to prepare mixed matrix membranes (MMMs), resulting in a significant enhancement in the adsorption selectivity of trichloroethylene (TCE) on membranes containing TMCS@silicalite-1 and TMDS@silicalite-1 particles. The experimental findings demonstrated that the PDMS membrane with a TMDS@silicalite-1 particle loading of 40 wt% exhibited the most favorable pervaporation performance. Under the conditions of a temperature of 30 °C, a flow rate of 100 mL min<sup>-1</sup>, and a vacuum degree of 30 kPa, the separation factor and total flux of a 3 × 10<sup>-7</sup> wt% TCE aqueous solution were found to be 139 and 242 g m<sup>-2</sup> h<sup>-1</sup>, respectively. In comparison to the unmodified silicalite-1/PDMS, the separation factor exhibited a 44% increase, while the TCE flux increased by 16%. Similarly, when compared to the pure PDMS membrane, the separation factor showed an 83% increase, and the TCE flux increased by 20%. These findings provide evidence that the hydrophobic modification of inorganic fillers can significantly enhance the separation performance of PDMS membranes for TCE.

Received 14th August 2023

Accepted 4th November 2023

DOI: 10.1039/d3ra05523j

[rsc.li/rsc-advances](http://rsc.li/rsc-advances)

### 1. Introduction

Trichloroethylene (TCE), a chlorinated solvent extensively employed in industrial manufacturing, has emerged as the most commonly identified volatile organic pollutant (VOC) in the environment, particularly in groundwater, due to improper disposal and other processes.<sup>1</sup> TCE possesses carcinogenic, teratogenic, and mutagenic properties, and can persist in underground aquifers for extended periods, posing a significant threat to both ecological security and human health. Nevertheless, conventional treatment approaches exhibit restricted removal efficacy and entail substantial operational expenses for TCE.<sup>2,3</sup> Consequently, there is an urgent requirement for an efficient and energy-conserving treatment technology.<sup>4–7</sup> Pervaporation (PV) technology is a highly efficient membrane separation technique that offers distinct advantages in the separation of organic/water systems and the dehydration of

organic solvents. This technology exhibits notable benefits, including low energy consumption, environmental compatibility, and unhindered gas–liquid equilibrium. Consequently, it holds great promise as a membrane technology for the separation of TCE/water systems.<sup>8,9</sup> The selectivity of the pervaporation membrane, as per the solution–diffusion model, mainly depends on the solubility properties of the feed solution within the MMMs.<sup>10,11</sup> The affinity of the membrane material to the permeate, which refers to the solubility of the permeate in the membrane, is determined by its chemical properties. Consequently, the selection of appropriate membrane materials plays a crucial role in improving the pervaporation separation efficiency (Fig. 1).

Polydimethylsiloxane (PDMS), a hydrophobic rubbery polymer with a low glass transition temperature, possesses the ability to create a continuous and uninterrupted channel internally, facilitating the diffusion of macromolecular organic substances. As a result, PDMS has emerged as the prevailing choice for pervaporation membrane materials.<sup>12</sup> Nevertheless, the PDMS film exhibits a thin thickness, resulting in inadequate mechanical properties and notable flaws during practical implementation. In order to address this issue, the

<sup>a</sup>School of Environmental and Municipal Engineering, Lanzhou Jiaotong University, Lanzhou 730070, China. E-mail: songxs@mail.lzjtu.cn

<sup>b</sup>Key Laboratory of Yellow River Water Environment in Gansu Province, Lanzhou Jiaotong University, No. 88 Anning West Road, Lanzhou 730070, China



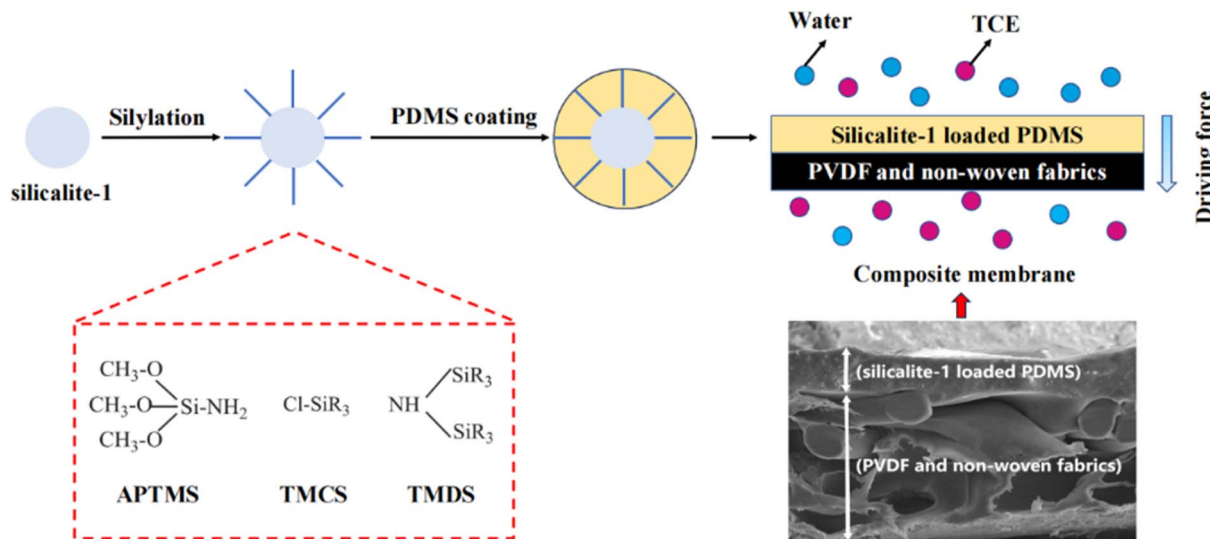


Fig. 1 Modification of silicalite-1 particles and preparation of composite membranes.

incorporation of hydrophobic particles into the PDMS polymer to form MMMs has emerged as a successful approach. In their study, Li *et al.*<sup>13</sup> conducted the synthesis of COF-300 and subsequently incorporated it into a PDMS matrix to create a mixed matrix membrane (MMM). Afterward, pure PDMS membranes were compared with the performance of the MMM. Specifically, the separation factor of PDMS membrane filled with COF-300 increased by 14.1% at 80 °C and 1 wt% furfural aqueous solution concentration. Conversely, the water permeability of the MMM decreased by 20%, leading to a furfural selectivity of 42.7%. Tian *et al.*<sup>14</sup> conducted a study in which they fabricated a PDMS mixed matrix membrane (MMM) incorporating hydrophobic carbon nanotubes (CNT). The K-MWCNT/PDMS MMM exhibited superior separation performance, particularly when the CNT loading was at 2 wt%. The separation factor experienced an increase from 9.1 to 10.4, while the permeation flux demonstrated a 50% enhancement (at temperatures ranging from 40 to 60 °C, with a feed ethanol concentration of 6 wt%). It is noteworthy that by increasing the hydrophobicity of the porous particles can increase the adsorption affinity of the MMM for organic matter, thereby leading to further improvements in the performance of the pervaporation system. Liu *et al.*<sup>15</sup> employed *n*-octyltriethoxysilane (OTES) as a means of grafting the *n*-octane chain onto the surface of ZSM-5 zeolite, thereby augmenting the hydrophobic properties of the zeolite. Subsequently, the tubular ceramic scaffold was coated with a PDMS solution containing ZSM-5 to fabricate the PDMS/ceramic composite membrane. Notably, the separation factor reached 14 when zeolite loading reached 40 wt%, representing an approximate doubling in comparison to the unfilled PDMS/ceramic composite membrane. Xue *et al.*<sup>16</sup> conducted an experiment where they incorporated ZSM-5 zeolite particles modified with coupling agent KH-570 into PDMS. This resulted in a significant enhancement of hydrophobicity in the composite membrane. The MMM has a separation factor of 24 and a total flux of

146.3 g m<sup>-2</sup> h<sup>-1</sup>, indicating a higher adsorption selectivity for butanol.

Silicalite-1, an aluminum-free MFI-type zeolite, has been developed for the purpose of separating organic substances from aqueous solutions due to its hydrophobic nature and its ability to selectively adsorb TCE in water systems.<sup>17</sup> To enhance PDMS membrane pervaporation performance, silicalite-1 has been investigated as a possible doping particle. Zhou *et al.*<sup>18</sup> synthesized dense MMM by incorporating vinyl-grafted silicalite-1 into polydimethylsiloxane (PDMS). This integration resulted in improved compatibility between silicalite-1 and PDMS, thereby increasing the selectivity of the ethanol solution. The modified silicalite-1/PDMS MMM exhibited a 49% increase in separation factor, reaching a value of 34.3, compared to the unmodified counterpart. Marthosa *et al.*<sup>19</sup> conducted a study in which they synthesized silicalite-1 zeolite and integrated it into a PDMS membrane on tetrafluoroethylene to evaluate its pervaporation performance in an ethanol solution. Based on a silicalite-1 content of 20 wt%, ethanol/water swelling increased from 1.33% to 1.52% compared to a PDMS membrane of pure material, and the separation factor rose from 2.55 to 5.56. However, there is a scarcity of research focused on enhancing the hydrophobicity of silicalite-1, which stands in contrast to the extensive body of literature on the modification of other conventionally doped zeolites.

In this study, silicalite-1 particles were incorporated into PDMS-based composite membranes in order to enhance their PV performance in TCE aqueous solutions. To achieve this, silicalite-1 particles were subjected to modification using silane coupling agents APTMS, TMCS, and TMDS, resulting in the formation of APTMS@silicalite-1, TMCS@silicalite-1, and TMDS@silicalite-1 particles. The morphological structure and hydrophobicity of the silane-modified silicalite-1 were assessed through SEM, FTIR, XRD, and water contact angle measurement, as depicted in Fig. 2. Subsequently, the aforementioned silicalite-1 particles were employed to fill PDMS in order to



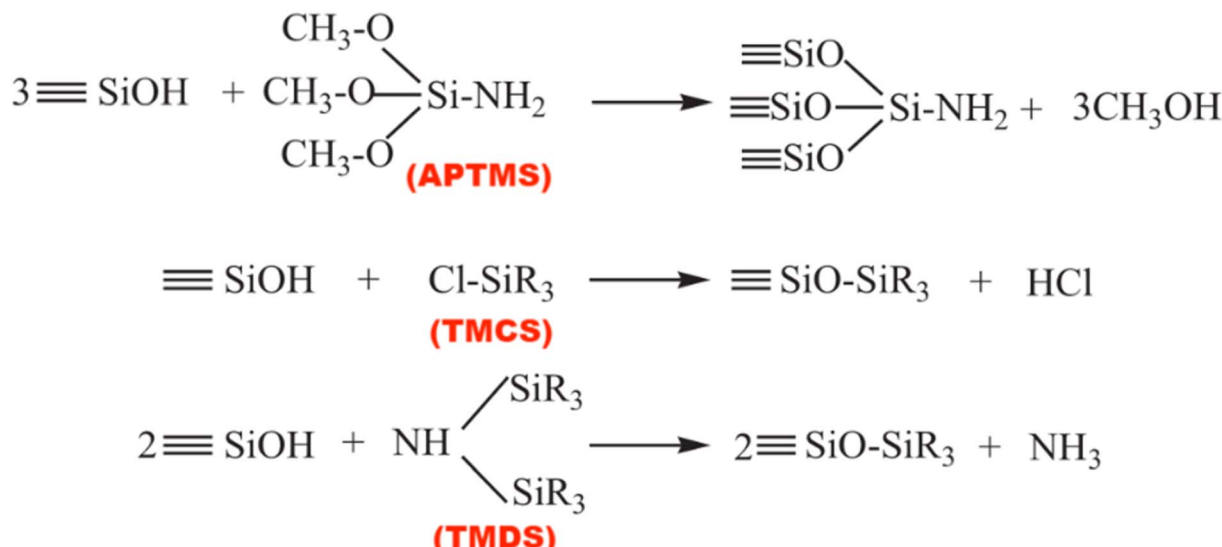


Fig. 2 Silicalite-1 hydrophobic modification schematic.

fabricate composite membranes, with the aim of enhancing the separation efficiency of said membranes for TCE aqueous solution. Furthermore, both preparation and operating conditions were examined to determine their impact on pervaporation.

## 2. Experimental

### 2.1. Materials

Trichloroethylene (TCE) standard solution was purchased from Beijing Hengxin Ruihua Technology Co., Ltd., China. *N,N*-Dimethylformamide (DMF) was purchased from Tianjin Damao Chemical Reagent Factory, China. *N*-Heptane, tetraethyl orthosilicate (TEOS), and dibutyltin dilaurate (DBDTL) were purchased from Fenlida Instruments Co., Ltd, China. 3-Aminopropyltrimethoxysilane (APTMS), trimethylchlorosilane (TMCS), and 1,1,3,3-tetramethyldisilazane (TMDS) were purchased from Shanghai Macklin Biochemical Technology Co., Ltd., China. Silicalite-1 zeolite (all-silicon) was purchased from Nankai Catalyst Factory, China. Polydimethylsiloxane (PDMS) (Silicone Rubber 107, Mw5000) was purchased from Shandong Laizhou Jintai Silicon Industry Co., Ltd., China. Polyvinylidene fluoride (PVDF) was purchased from Shandong Xiya Chemical Co., Ltd., China.

### 2.2. Hydrophobic modification of silicalite-1 zeolite

The surface of silicalite-1 zeolite underwent hydrophobic modification using APTMS, TMCS, and TMDS silane coupling agents, resulting in the formation of APTMS@silicalite-1, TMCS@silicalite-1, and TMDS@silicalite-1 modified zeolite particles. Prior to utilization, silicalite-1 particles were calcined at 600 °C for 4 hours in a muffle furnace. Subsequently, the particles were dried in an oven at 120 °C overnight to ensure complete removal of any template residues. The silicalite-1 particles and modifier (APTMS, TMCS, or TMDS) were dispersed in *n*-heptane (with a weight ratio of  $W_{\text{silicalite-1}}$ :

$W_{\text{modifier}} : W_{n\text{-heptane}} = 1 : 2 : 75$ ) for the purpose of surface modification.<sup>20</sup> Afterwards, the mixture was centrifuged and washed with *n*-heptane during the next 24 hours, in order to separate the unreacted modifiers. The resulting silane-modified silicalite-1 zeolite were then dried at 20 °C for five hours and subsequently subjected to vacuum heating at 250 °C for three hours.

### 2.3. Fabrication of MMMs

Preparation of PVDF carrier.<sup>21</sup> PVDF is an ideal porous carrier material because of its excellent chemical stability, hydrophobicity, and film-forming properties, and it is easily processed into a support membrane with high permeability. A solution containing a specific quantity of PVDF was prepared by dissolving it in DMF with a concentration of 11 wt%. The solution was then subjected to stirring at room temperature for a duration of 8 hours. A membrane maker was then used to flatten the solution onto a nonwoven fabric. Immediately following this step, the resulting membrane was immersed in water at 25 °C for a brief period of 2 seconds before being removed. The membrane was then dried in a fume hood for a duration of 30 minutes, resulting in the formation of an ultra-porous PVDF membrane.<sup>21</sup> The preparation process of a mixed casting solution containing ZSM-5 loaded PDMS involved dissolving PDMS and TEOS in *n*-heptane and stirring for 2 hours. The modified zeolite particles were introduced and agitated at ambient temperature for a duration of 1 hour. Subsequently, a specific quantity of catalyst DBDTL was incorporated, continuously agitated at ambient temperature for 30 minutes, and subsequently subjected to ultrasonic treatment for 30 minutes to mitigate agglomeration and eliminate foam from the solution. The proportions of polymer, solvent, crosslinking agent, and catalyst were established as  $W_{\text{PDMS}} : W_{n\text{-heptane}} : W_{\text{TEOS}} : W_{\text{DBDTL}} = 30 : 70 : 2.5 : 0.5$  (g) in accordance with the experimental design.<sup>22,23</sup> The preparation of the silicalite-1/PDMS/PVDF MMMs involved the utilization of the solution casting



method. Specifically, silicalite-1/PDMS mixed casting solution was applied for one minute to the PVDF substrate membrane's external surface, after which it was transferred to a fume hood. Subsequently, the solvent was allowed to evaporate for 24 hours at ambient temperature, followed by 12 hours of curing in a vacuum oven at 120 °C. Ultimately, the modified silicalite-1/PDMS/PVDF MMMs were successfully prepared.

#### 2.4. Characterization

To analyze the morphology of silicalite-1 particles and composite membranes, high-resolution SEM images were obtained at an accelerating voltage of 2 kV using scanning electron microscopy (SEM, Gemini SEM 500, Carl Zeiss, Germany). Infrared spectroscopy (FTIR, VERTEX 70, Brook, Germany) was performed in the range of 4000–400  $\text{cm}^{-1}$  to analyze the changes in the chemical structures before and after cross-linking, such as the changes in functional groups. X-ray diffractometry (XRD, XRD-7000L, Brook, Germany) was used to characterize the silicalite-1 particles, and the changes in diffraction peak intensity and crystallinity were investigated. The changes in the hydrophilicity and hydrophobicity of the composite membranes and silicalite-1 particles were observed by a video optical contact angle measuring instrument (OCA25, Brook, Germany). The composite membrane was cut into 20 mm  $\times$  20 mm samples, and 2  $\mu\text{L}$  of deionized water was dropped on the surface of each sample for water contact angle testing. An average value was determined for each sample by measuring three different points. The error range was  $\pm 0.6^\circ$ .

#### 2.5. PV experiment

The PV apparatus is schematically illustrated in Fig. 3. Our PV experiments were performed using a laboratory-scale

membrane system with an effective membrane area of  $2.46 \times 10^{-3} \text{ m}^2$  and a permeate pressure of 30 kPa. The feed solution between the feed tank and membrane cell was circulated at 100  $\text{mL min}^{-1}$ . The vacuum pressure on the permeate side was controlled by a vacuum pump. When the operation reached a steady state, liquid nitrogen condensation to collected permeate vapor samples. A headspace chromatography-mass spectrometer (GC-MS 7000C, Agilent, USA) was used to analyze these samples quantitatively and qualitatively.

The permeation flux ( $J$ ) and separation factor ( $\alpha$ ) were calculated as follows:<sup>24</sup>

$$J = M/(A \times t) \quad (1)$$

$$\alpha = (y_{\text{TCE}}/y_{\text{water}})/(x_{\text{TCE}}/x_{\text{water}}) \quad (2)$$

where  $M$  is the total amount of permeate collected during the experimental time interval  $t$  of 1 h at steady state,  $A$  is the effective membrane area,  $x$  and  $y$  represent the mole fraction of a component in the permeate and the feed, respectively.

### 3. Results and discussion

#### 3.1. Characterization of silane-modified silicalite-1

The morphology of silicalite-1 particles before and after modification is shown in Fig. 4. The silicalite-1 particles that underwent silane modification exhibited a cuboid crystal structure, which closely resembled that of the unmodified silicalite-1 particles. Therefore, the introduction of the modifier did not significantly alter the morphology of the zeolite particles.<sup>18</sup>

The results of the FTIR spectrum are presented in Fig. 5. In the unmodified silicalite-1 spectrum, a weak stretching

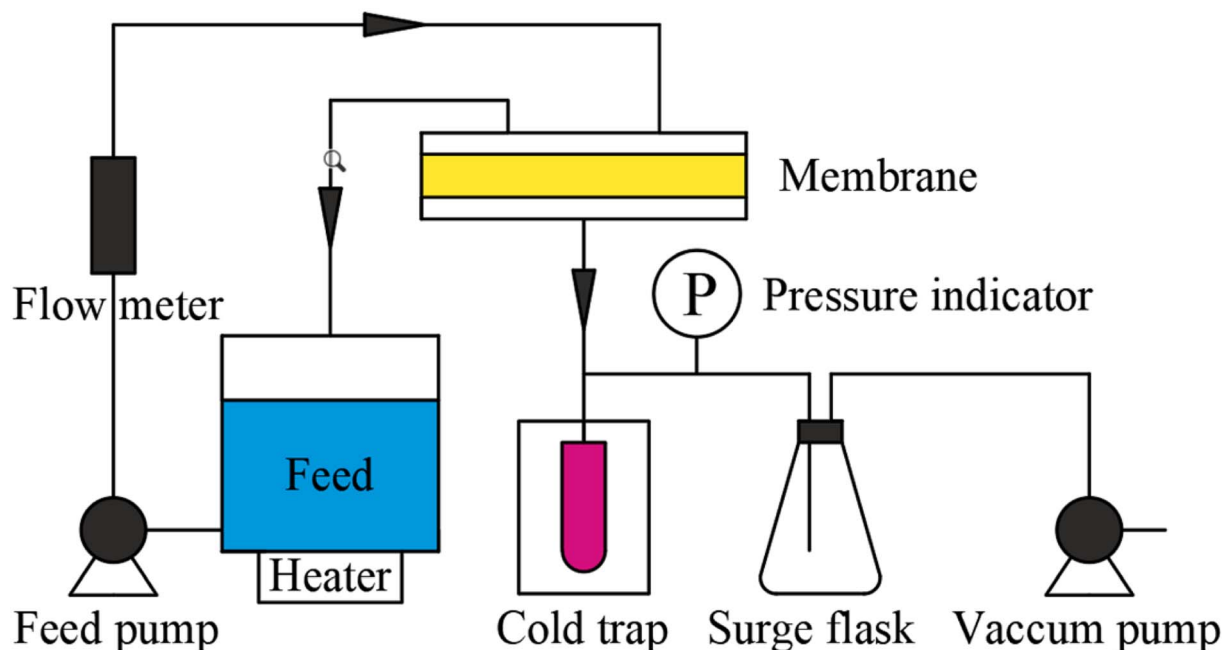


Fig. 3 Schematic diagram of pervaporation apparatus.



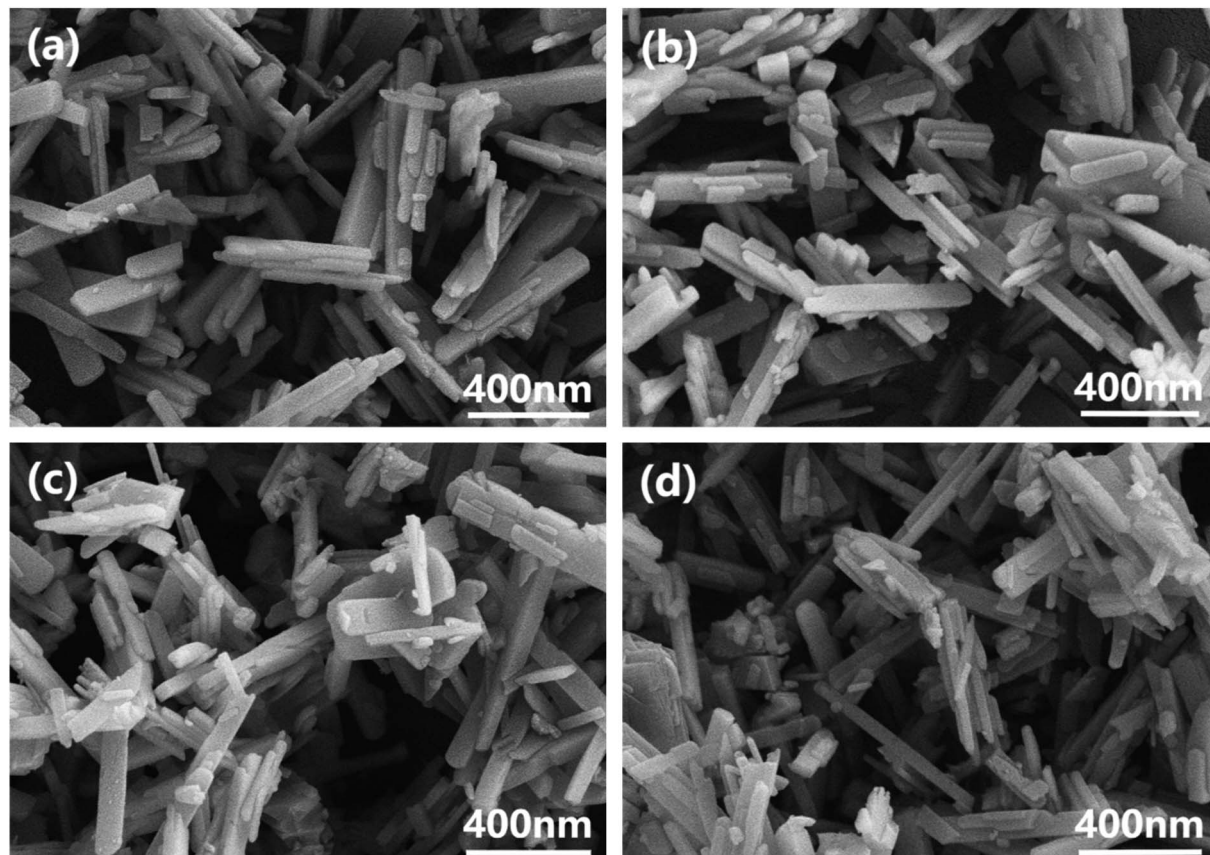


Fig. 4 SEM images of (a) unmodified silicalite-1, (b) APTMS@silicalite-1, (c) TMCS@silicalite-1, and (d) TMDS@silicalite-1.

vibration of the  $-\text{OH}$  group is observed at  $3450\text{ cm}^{-1}$ . However, the intensity of the  $-\text{OH}$  group vibration peak decreases in the modified silicalite-1 spectrum. This decrease can be attributed to the condensation reaction between silicalite-1 particles and the silane coupling agent.<sup>18</sup> Additionally, in the FTIR spectra of modified silicalite-1, the characteristic peaks at  $2960\text{ cm}^{-1}$  and

$2870\text{ cm}^{-1}$  correspond to the asymmetric tensile vibration of  $-\text{CH}_3$ , which originates from the methyl groups present in the silane coupling agent.<sup>20</sup> This observation indirectly substantiated the grafting of APTMS, TMCS, and TMDS onto the surface of silicalite-1 particles, respectively. Modified silicalite-1 particles typically exhibit a prominent peak at  $1095\text{ cm}^{-1}$  indicative of  $\text{Si}-\text{O}-\text{Si}$  asymmetric stretching.<sup>25</sup>

Fig. 6 presents X-ray diffraction (XRD) results. Within the  $2\theta$  range of  $22^\circ$  to  $26^\circ$ , all four crystals exhibited prominent peaks, with the MFI-type characteristic peak of the MFI structure being the most intense. This suggests that both the pre-modified and post-modified silicalite-1 particles possess the structure of an MFI-type molecular sieve.<sup>26</sup> Furthermore, the modified silicalite-1 shows the same characteristic peaks as the unmodified silicalite-1, and no impurity peaks are evident. These findings indicate that the crystal structure of the modified silicalite-1 remains unchanged.

Silicalite-1 molecular sieve is hydrophobic due to its alkylation modification. Consequently, the alteration in hydrophobicity can be observed by measuring the contact angle of the molecular sieve modified with various silane coupling agents, as depicted in Fig. 7. The unmodified silicalite-1 exhibits a water contact angle of  $96.1^\circ$ , whereas APTMS@silicalite-1 and TMCS@silicalite-1 demonstrate water contact angles of approximately  $85.2^\circ$  and  $101.9^\circ$ , respectively. Notably, TMDS@silicalite-1 exhibits a significantly higher water contact

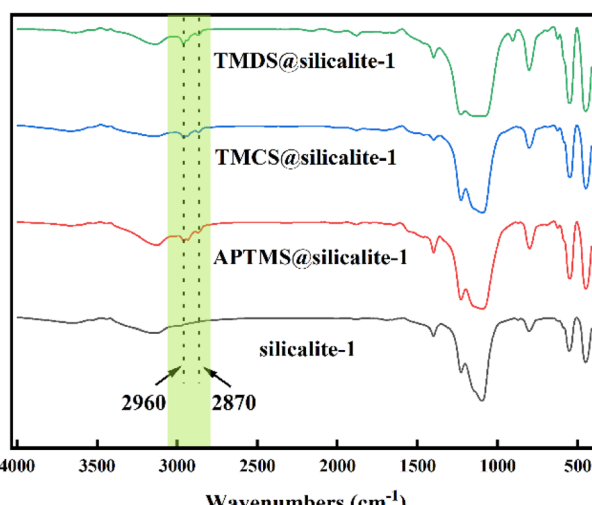


Fig. 5 FTIR spectra of unmodified silicalite-1, APTMS@silicalite-1, TMCS@silicalite-1, and TMDS@silicalite-1.

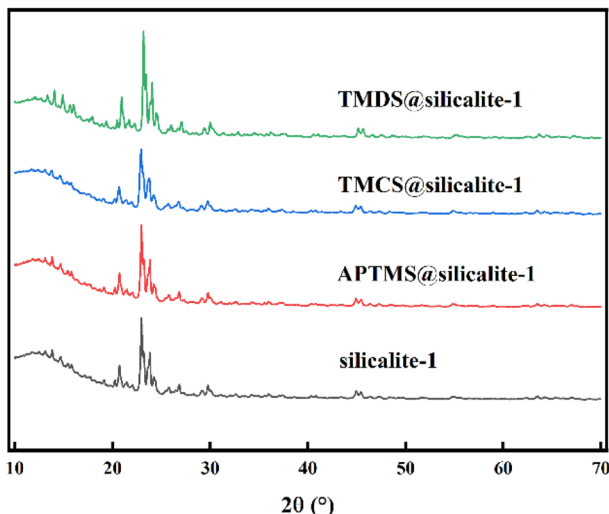


Fig. 6 XRD patterns of unmodified silicalite-1, APTMS@silicalite-1, TMCS@silicalite-1, and TMDS@silicalite-1.

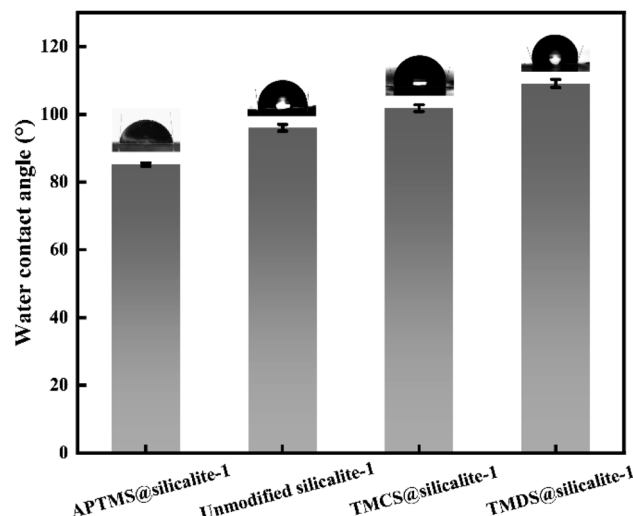


Fig. 7 Water contact angles of APTMS@silicalite-1, unmodified silicalite-1, TMCS@silicalite-1, and TMDS@silicalite-1.

angle of  $109.1^\circ$ . Among them, the surface of APTMS modified silicalite-1 has a hydrophilic group- $\text{NH}_2$ , so its water contact angle decreases compared with the unmodified silicalite-1 particles. The increase of  $-\text{CH}_3$  on the surface of silicalite-1 modified by TMCS and TMDS leads to the increase of water contact angle. Notably, the silicalite-1 zeolite modified by TMDS demonstrates the highest level of hydrophobicity. This can be attributed to the more compact surface structure of the TMDS-modified silicalite-1 zeolite, which in turn results in the largest contact angle and the most pronounced hydrophobicity.<sup>27</sup>

### 3.2. Characterization and PV performance of the MMMs

The SEM images in Fig. 8 depict the cross-sections of silicalite-1/PDMS MMMs before and after modification. Both the modified and unmodified silicalite-1/PDMS MMMs, containing a particle

loading of 20 wt%, exhibit similar morphology and thickness, with no discernible defects. Notably, the unmodified silicalite-1/PDMS MMMs display an uneven surface (Fig. 8a), while the modified silicalite-1/PDMS MMMs exhibit a smooth surface (Fig. 8b and c). This phenomenon arises from the lack of compatibility between PDMS material and silicalite-1 particles, leading to PDMS phase contains an uneven distribution of inorganic silicalite-1 particles. The incorporation of a silane coupling agent as an intermediary between silicalite-1 and PDMS facilitates the blending of the organic and inorganic phases, thereby enhancing the crystalline characteristics of the mixed matrix membranes (MMMs).<sup>28</sup>

The alteration of hydrophilicity and hydrophobicity on the surface of the MMMs after the introduction of modified silicalite-1 molecular sieve into PDMS can be more effectively assessed by the water contact angle, as depicted in Fig. 9. The water contact angle of unmodified silicalite-1/PDMS MMM was measured at  $120.7^\circ$ . However, upon incorporating TMCS and TMDS modified silicalite-1/PDMS MMMs, the water contact angle increased significantly to  $123.8^\circ$  and  $124.2^\circ$ , respectively, indicating a notable enhancement in hydrophobicity. The hydrophobicity of the APTMS modified silicalite-1/PDMS MMM is marginally lower compared to the unmodified composite membrane, owing to the presence of the hydrophilic group- $\text{NH}_2$  introduced by APTMS.<sup>29</sup> The findings indicate that the inclusion of TMCS@silicalite-1 and TMDS@silicalite-1 particles significantly enhance the hydrophobicity of the composite membrane surface, thereby positively impacting the PV performance of the MMMs.

The pervaporation performance of silicalite-1/PDMS MMMs (with a zeolite addition of 20 wt%) was investigated before and after modification under specific conditions, including a feed TCE concentration of  $3 \times 10^{-7}$  wt%, a feed temperature and flow rate were  $30^\circ\text{C}$  and  $100 \text{ mL min}^{-1}$ , the vacuum degree is  $30 \text{ kPa}$ . Fig. 10 illustrates the results. It was observed that the APTMS modified silicalite-1/PDMS MMM exhibited a lower separation factor compared to the unmodified MMM, although the total flux increased. On the other hand, the separation factor of the silicalite-1/PDMS MMM modified by TMCS and TMDS showed an increase compared to the unmodified MMM. Simultaneously, a decline in the overall flux was observed (Fig. 10a). This can be attributed to the grafting of the hydrophilic group- $\text{NH}_2$  onto the surface of the APTMS@silicalite-1 particles, causing the hydrophobicity of the particles to decrease and consequently diminishing the preferential adsorption of TCE by the composite membrane. As a consequence, the separation factor decreases, while the hydrophilic group facilitates the passage of a substantial number of water molecules (Fig. 10b), leading to a significant increase in membrane flux.<sup>29</sup> The TMCS@silicalite-1 and TMDS@silicalite-1 molecular sieves exhibit an elevated hydrophobic angle attributed to the inclusion of surface alkyl groups. This augmentation enhances the surface hydrophobicity of the composite membrane, resulting in a reduction in water flux and a heightened affinity for TCE molecules. Consequently, the separation factor of the composite membrane experiences a gradual increase.<sup>30</sup> Hence, the application of silane



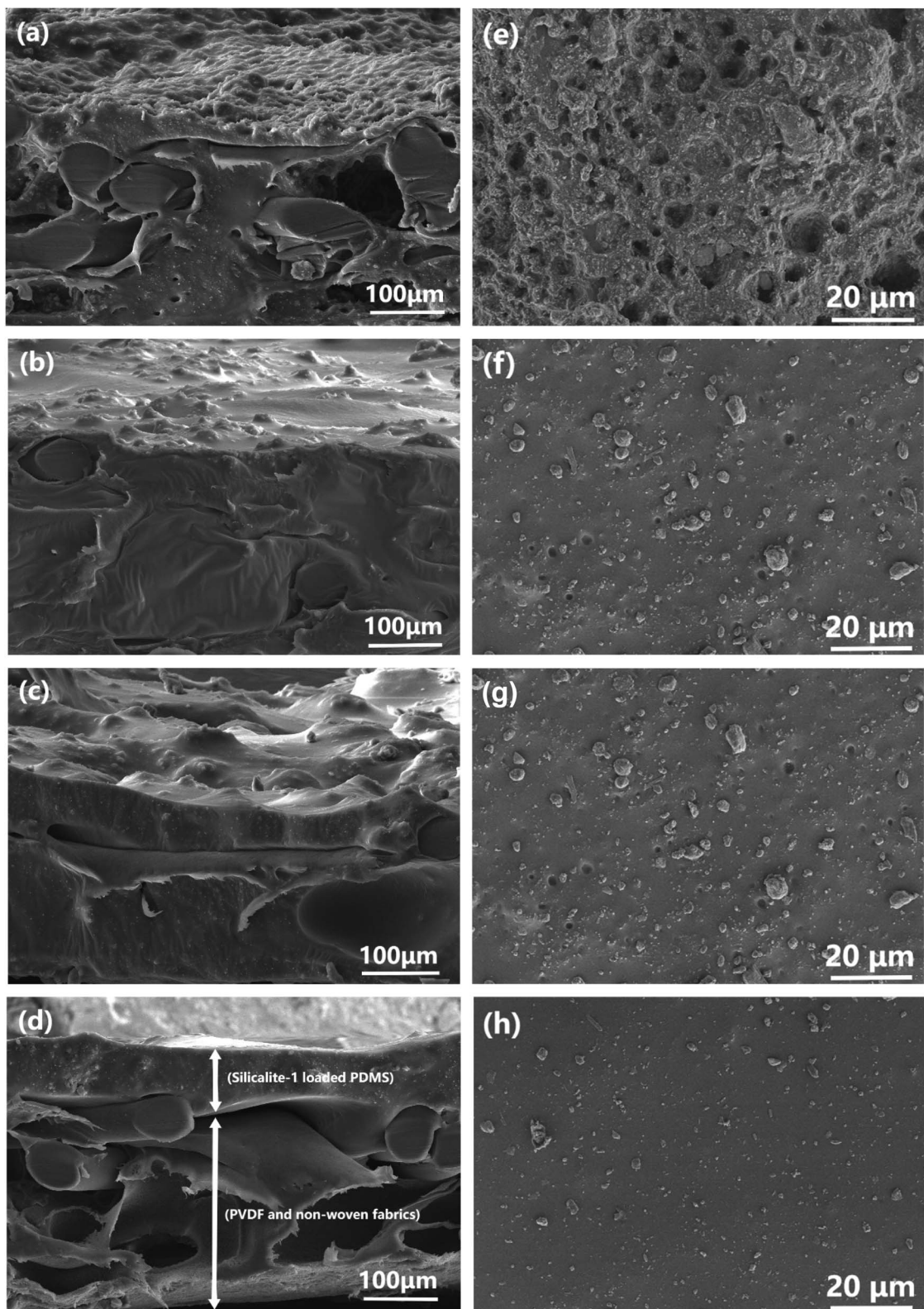


**Fig. 8** Cross-section images of the MMMs doped with 20 wt% (a) unmodified silicalite-1, (b) APTMS@silicalite-1, (c) TMCS@silicalite-1 and (d) TMDS@silicalite-1 particles; surface images of the MMMs doped with 20 wt% (e) unmodified silicalite-1, (f) APTMS@silicalite-1, (g) TMCS@silicalite-1 and (h) TMDS@silicalite-1 particles.

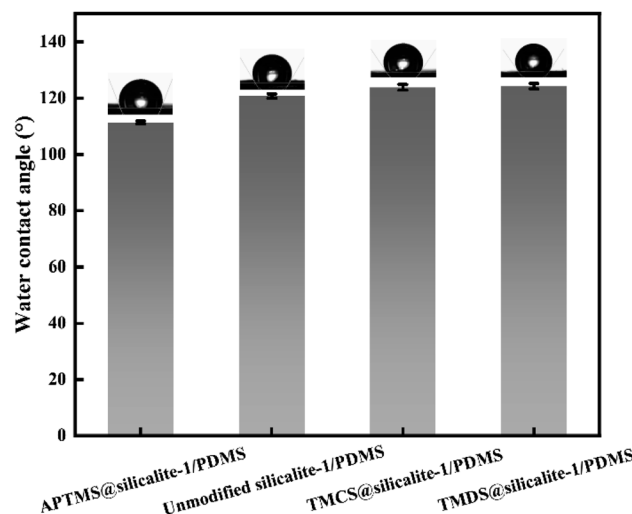


Fig. 9 Water contact angles of the MMMs doped with 20 wt% APTMS@silicalite-1, unmodified silicalite-1, TMCS@silicalite-1 and TMDS@silicalite-1 particles.

modification on the silicalite-1 zeolite molecular sieve demonstrates a notable enhancement in the PV performance of the PDMS MMMs. Notably, the TMDS@silicalite-1 composite exhibits the most substantial hydrophobic angle, leading to the most pronounced improvement in membrane separation performance and the highest pervaporation efficiency for TCE aqueous solution. Consequently, further investigations will be conducted on the TMDS@silicalite-1/PDMS mixed matrix membrane (MMM) to explore its potential.

### 3.3. Effect of zeolite loading on TMDS@silicalite-1/PDMS MMMs

The scanning electron microscopy (SEM) cross-section of TMDS@silicalite-1/PDMS MMMs with varying zeolite loadings

is depicted in Fig. 11. The smooth and uniform surface of the pure PDMS membrane was observed. However, with an increase in the amount of TMDS@silicalite-1 molecular sieve to 20 wt%, the composite membrane displayed molecular sieve agglomeration bulges that were unevenly distributed, resulting in a notable increase in surface roughness (Fig. 11c). At a concentration of 40 wt% of TMDS@silicalite-1 molecular sieve (Fig. 11e), a significant reduction in molecular sieve agglomeration was observed, resulting in a more uniform distribution. Furthermore, as particle loading increased, the surface of MMMs exhibited a gradual roughening, without any noticeable defects.

The water contact angle test results for TMDS@silicalite-1/PDMS MMMs with varying amounts of molecular sieve additions are presented in Fig. 12. The water contact angle of the pure PDMS membrane was measured to be 117.2°. Upon incorporation of the TMDS@silicalite-1 particles, the surface hydrophobicity of the composite membrane was enhanced, and this enhancement continued to increase with higher amounts of molecular sieve addition. When the weight percentage of TMDS@silicalite-1 molecular sieve is 40%, the hydrophobic angle can achieve a value of 137°. The findings indicate that the incorporation of a hydrophobic molecular sieve significantly alters the hydrophilic and hydrophobic properties of the composite membrane surface, thereby enhancing the MMM's ability to adsorb TCE.<sup>31</sup>

The impact of TMDS@silicalite-1 particle loading on the pervaporation performance of PDMS MMMs was examined under specific conditions, including a feed TCE concentration of  $3 \times 10^{-7}$  wt%, a feed temperature and flow rate were 30 °C and 100 mL min<sup>-1</sup>, the vacuum degree was 30 kPa, as depicted in Fig. 13. Analysis of Fig. 13a reveals that as the loading of TMDS@silicalite-1 particles increase from 0 wt% to 40 wt%, the separation factor gradually rises, peaking at 139 when the addition amount reaches 50 wt%, while the total flux exhibits a consistent downward trend. The rationale behind this

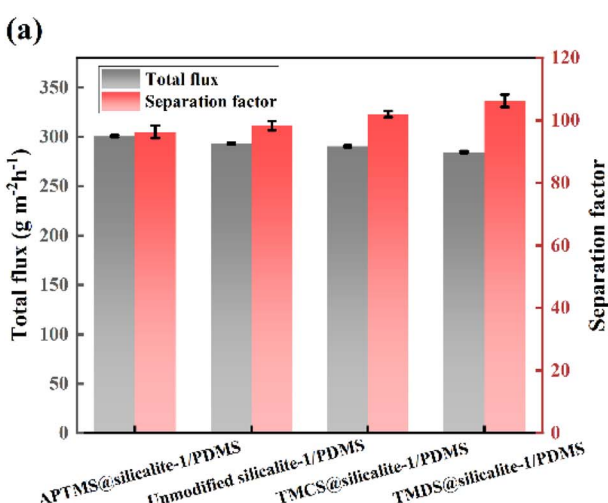
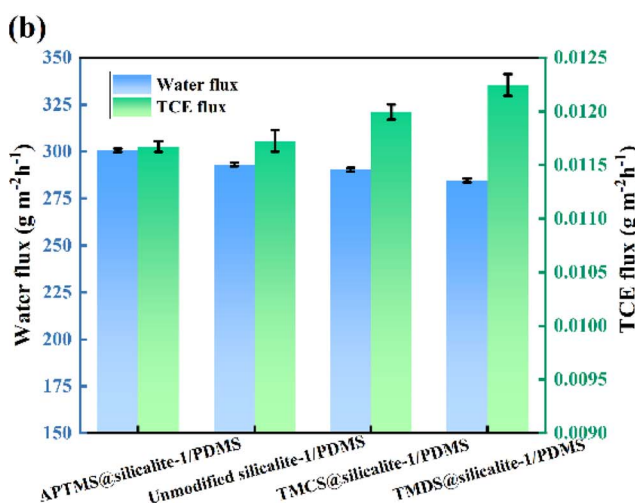


Fig. 10 PV performances of the MMMs doped with APTMS@silicalite-1, unmodified silicalite-1, TMCS@silicalite-1, and TMDS@silicalite-1 particles in a  $3 \times 10^{-7}$  wt% TCE solution at 30 °C.



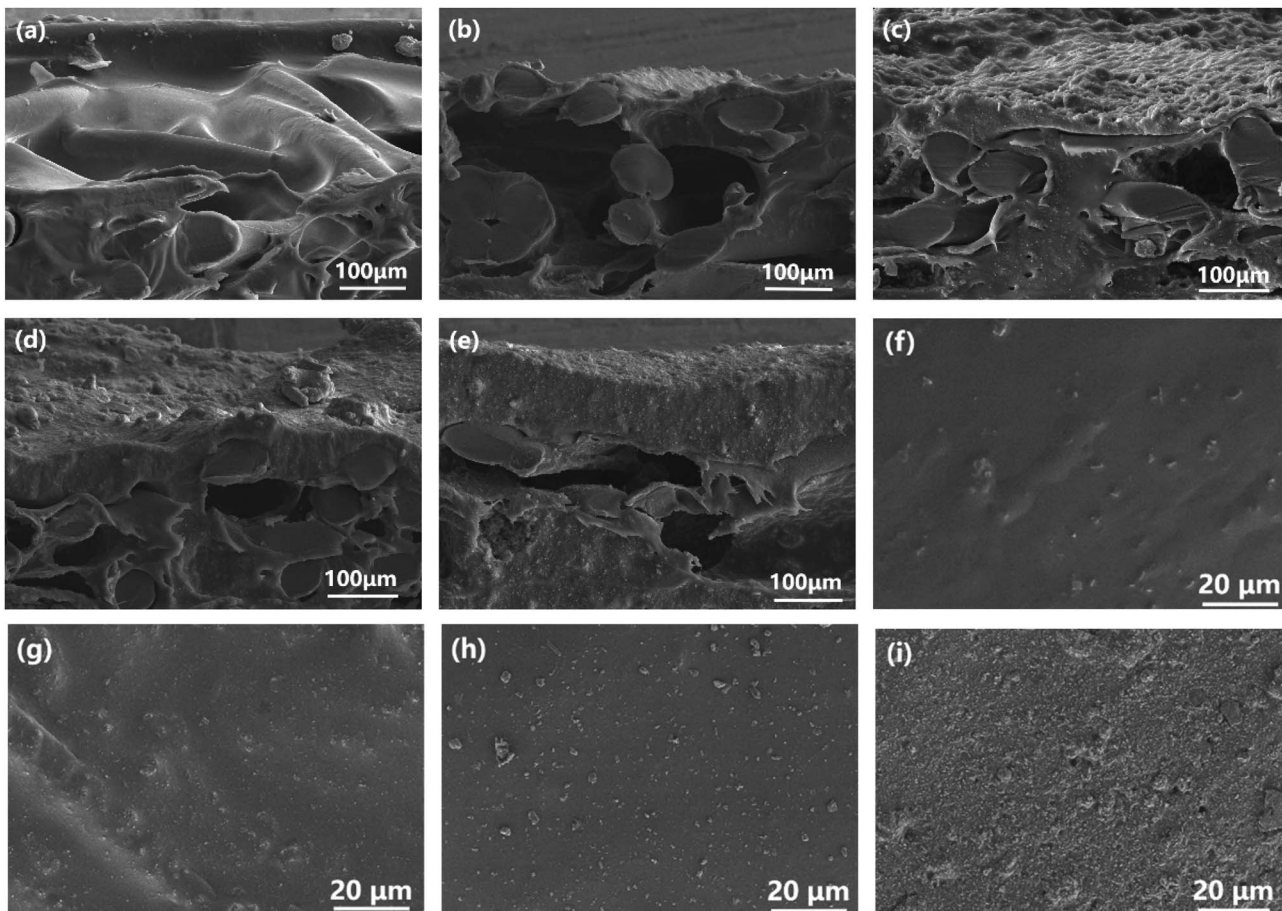


Fig. 11 Cross-section images of TMDS@silicalite-1/PDMS membranes with different particle loading amounts: (a) 0 wt%, (b) 10 wt%, (c) 20 wt%, (d) 30 wt% and (e) 40 wt%; surface images of TMDS@silicalite-1/PDMS membranes with different particle loading amounts: (f) 0 wt%, (g) 10 wt%, (h) 20 wt%, (i) 30 wt.

phenomenon lies in the direct correlation between the quantity of TMDS@silicalite-1 molecular sieve and the loading of molecular sieve within the PDMS separation layer. This increase

in loading results in an augmented presence of hydrophobic channels within the composite membrane, thereby facilitating the preferential adsorption and diffusion of TCE molecules.<sup>32</sup> Consequently, the TCE flux exhibits a consistent upward trajectory (as depicted in Fig. 13b), accompanied by an enhanced selectivity. However, it is important to note that the presence of TMDS@silicalite-1 molecular sieve concurrently impedes the movement between PDMS molecular chains, thereby diminishing its free volume. The hindering impact becomes more evident as the molecular sieve content increases, leading to an increase in mass transfer resistance for water molecules.<sup>19</sup> Furthermore, as the loading of TMDS@silicalite-1 particles increase, the surface hydrophobicity of the composite membrane also increases gradually, resulting in a significant decrease in water flux (Fig. 13b) and consequently reducing the total flux. The findings indicate that the TMDS@silicalite-1/PDMS MMM with a zeolite loading of 40 wt% exhibits the most favorable pervaporation separation performance for a  $3 \times 10^{-7}$  wt% TCE aqueous solution. The separation factor and TCE flux reach 139 and  $0.014 \text{ g m}^{-2} \text{ h}^{-1}$ , respectively, 45% and 16% higher than unmodified silicalite-1/PDMS MMM.

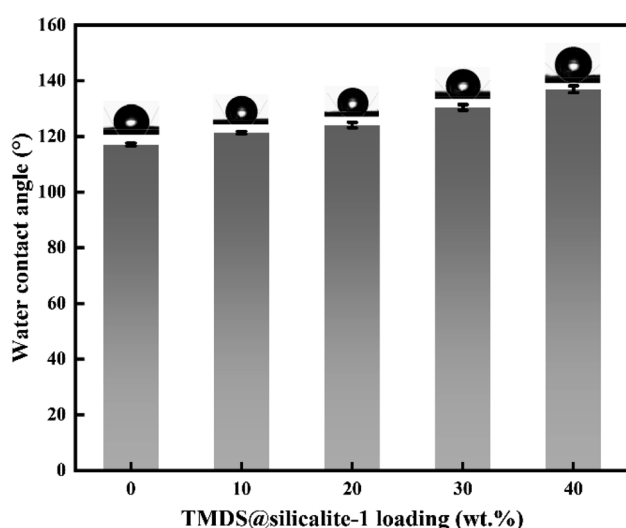


Fig. 12 Water contact angles of TMDS@silicalite-1/PDMS membranes with different particle loading amounts.



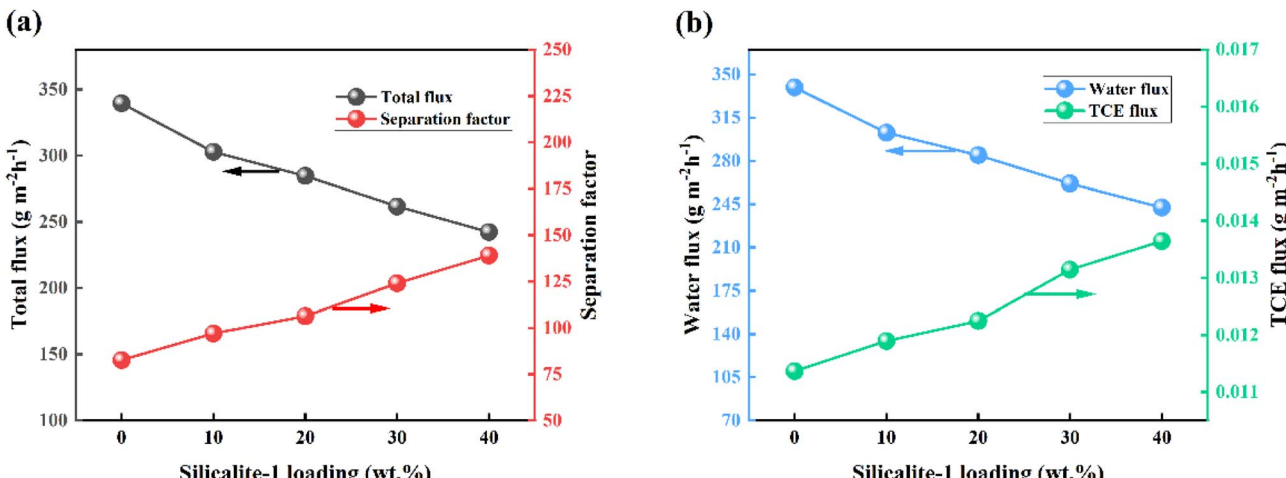


Fig. 13 PV performance of TMDS@silicalite-1/PDMS membranes with different particle loading amounts. (a) Effects on total flux and separation factor, (b) effect on water flux and TCE flux.

### 3.4. Effect of feed concentration on PV performance

The PV performance of TMDS@silicalite-1/PDMS MMM was examined to determine the impact of feed TCE concentration ranging from  $1 \times 10^{-7}$  wt% to  $5 \times 10^{-7}$  wt%. The investigation was conducted under specific conditions, including a feed temperature and flow rate were  $30^\circ\text{C}$  and  $100 \text{ mL min}^{-1}$ , the vacuum degree was 30 kPa, as depicted in Fig. 14. The separation factor of the MMMs decreased with increasing TCE concentration in the feed solution. Conversely, a higher concentration of TCE molecules in the feed solution led to an increase in the total flux (Fig. 14a) due to the increased presence of TCE molecules in the selective layer of the MMM. The organic solvent exhibits a distinct capacity for dissolving the polymer, thereby rendering the membrane surface more susceptible to swelling. Therefore, the PDMS chain interaction force is diminished, resulting in the voids becoming larger. Consequently, smaller water molecules can traverse more easily,

resulting a decrease in the separation factor of the composite membrane.<sup>33,34</sup> Simultaneously, as the pores of the selective layer on the membrane surface increase, the impediment to mass transfer also diminishes. Consequently, the permeation rate of TCE molecules and water molecules accelerates, leading to a gradual augmentation in TCE flux and water flux (Fig. 14b), thereby causing an upward trajectory in the overall flux of the composite membrane.

### 3.5. Effect of feed temperature on PV performance

The pervaporation performance of TMDS@silicalite-1/PDMS MMM was examined to determine the impact of feed temperature (ranging from  $20^\circ\text{C}$  to  $60^\circ\text{C}$ ) under specific conditions, including a feed TCE concentration and flow rate were  $3 \times 10^{-7}$  wt% and  $100 \text{ mL min}^{-1}$ , the vacuum degree was 30 kPa. Fig. 15 illustrates the results, indicating that the separation factor exhibits an increasing trend as the temperature rises. At

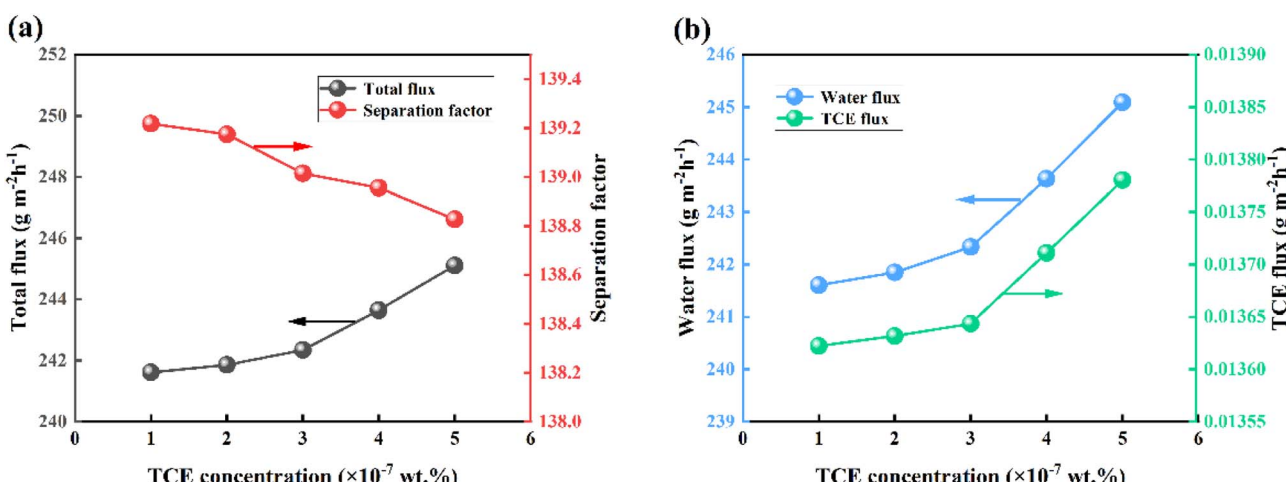


Fig. 14 Effect of feed concentration on PV performance of TMDS@silicalite-1/PDMS membranes with 40 wt% loading for  $3 \times 10^{-7}$  wt% TCE solution. (a) Effects on total flux and separation factor, (b) effect on water flux and TCE flux.

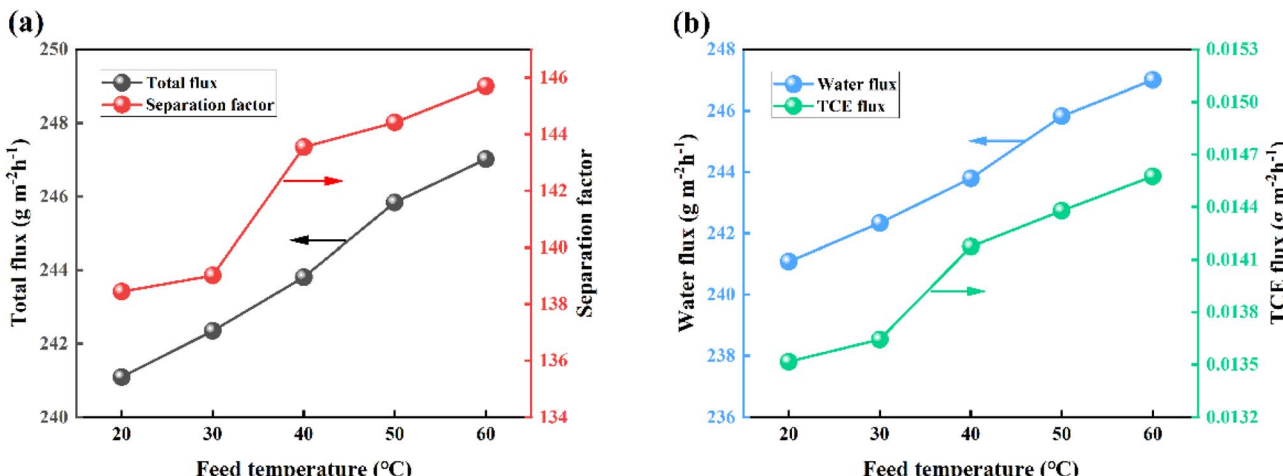


Fig. 15 Effect of feed temperature on PV performance of TMDS@silicalite-1/PDMS membranes with 40 wt% loading for  $3 \times 10^{-7}$  wt% TCE solution. (a) Effects on total flux and separation factor, (b) effect on water flux and TCE flux.

an operating temperature of 60 °C, the separation factor can attain a value of 146. This phenomenon can be attributed to the higher permeation activation energy of TCE compared to water, as well as the greater influence of temperature on TCE compared to water.<sup>35,36</sup> Consequently, an increase in operating temperature leads to a more pronounced alteration in TCE flux compared to water flux. Consequently, the concentration of TCE in the permeate exhibits an upward trend with rising temperature. Furthermore, the elevation in temperature can augment the disparity in vapor partial pressure across the membrane, thereby intensifying the molecular thermal motion within the pervaporation membrane. This phenomenon ultimately enhances the membrane's selectivity towards the separated components.<sup>37</sup> Simultaneously, the temperature increment also leads to an increase in the overall flux of the MMMs. This can be attributed to the heightened thermal motion of the polymer chains, which facilitates the solution's permeation, consequently resulting in amplified water flux and TCE flux (Fig. 15b).

### 3.6. Effect of feed flow rate on PV performance

The impact of varying feed flow rates on the pervaporation efficiency of TMDS@silicalite-1/PDMS MMMs was examined under specific conditions, including a feed TCE concentration and temperature were  $3 \times 10^{-7}$  wt% and 30 °C, the vacuum degree was 30 kPa, as depicted in Fig. 16. The findings indicated that the overall membrane flux, water flux, TCE flux, and separation factor exhibited a gradual increase with the augmentation of feed flow rate, albeit the magnitude of change was minimal. This phenomenon can be attributed to the acceleration of the flow rate, resulting in a reduction in the thickness of the boundary layer and a weakening of concentration polarization, thereby facilitating the mass transfer of TCE.<sup>38</sup> Furthermore, the increase in flow rate leads to a transition towards turbulent flow in the feed fluid, intensifying the degree of this flow state. Consequently, there is an augmented contact between TCE and the composite membrane, promoting the interaction between the membrane and TCE, which further enhances the permeation of the permeation component.<sup>39</sup>

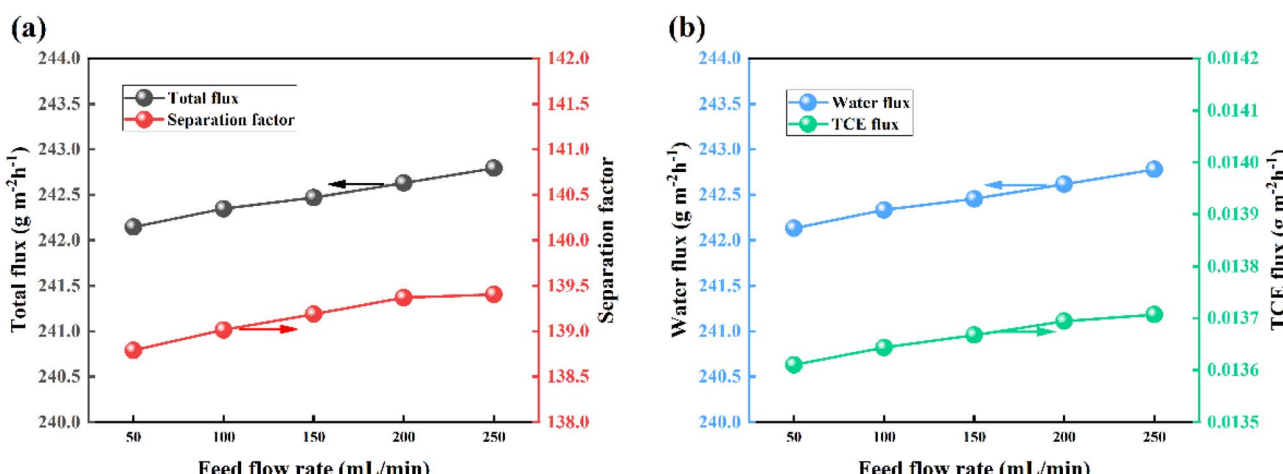


Fig. 16 Effect of feed flow rate on PV performance of TMDS@silicalite-1/PDMS membranes with 40 wt% loading for  $3 \times 10^{-7}$  wt% TCE solution. (a) Effects on total flux and separation factor, (b) effect on water flux and TCE flux.



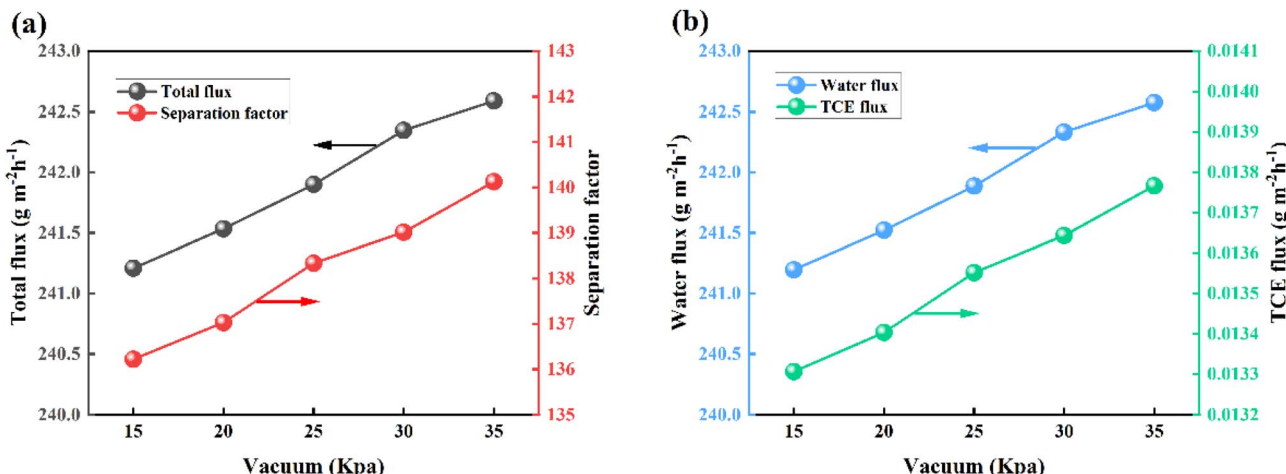


Fig. 17 Effect of permeate-side on PV performance of TMDS@silicalite-1/PDMS membranes with 40 wt% loading for  $3 \times 10^{-7}$  wt% TCE solution. (a) Effects on total flux and separation factor, (b) effect on water flux and TCE flux.

Table 1 PV performance of TCE separated by different membranes

Membrane	Feed concentration (wt%)	Feed temperature (°C)	Particle loading (wt%)	Separation factor	Total flux ( $\text{g m}^{-2} \text{h}^{-1}$ )	Reference
Silicalite-1	$1 \times 10^{-4}$	30	—	10	4	42
Polyvinyl acetate	$4.57 \times 10^{-4}$	25	—	110	310	43
Poly(acrylate-co-acrylic)	$2.01 \times 10^{-1}$	25	—	108	638	44
PDMS	$2.4 \times 10^{-4}$	55	—	104	400	29
Silicalite-1@TMDS/PDMS	$3 \times 10^{-7}$	30	40	139	242	This work

### 3.7. Effect of vacuum degree on PV performance

The pervaporation performance of TMDS@silicalite-1/PDMS MMM was investigated under specific conditions, including a feed TCE concentration of  $3 \times 10^{-7}$  wt%, a feed temperature and flow rate were 30 °C and 100 mL min<sup>-1</sup>. The effect of vacuum degree (ranging from 15 kPa to 35 kPa) on the pervaporation performance was examined, as depicted in Fig. 17. It was observed that as the vacuum degree on the permeation side increased, both the total flux and the separation factor exhibited an upward trend. This phenomenon occurs due to the maintenance of atmospheric pressure in the upstream of the membrane, resulting in a gradual increase in the vacuum degree downstream of the membrane. Consequently, the pressure difference between the upstream and downstream sides of the membrane increases, thereby enhancing the driving force of membrane pervaporation. As a result, the mass transfer resistance of the permeation component within the membrane is reduced, resulting in an increase in overall flux.<sup>40</sup> Furthermore, due to the higher saturated vapor pressure of TCE compared to water, the TCE molecules exhibit a significantly stronger driving force when the vacuum level on the permeate side is elevated. Consequently, this phenomenon leads to an improved selectivity and separation factor of the membrane (Table 1).<sup>41</sup>

## 4. Conclusion

In this study, the objective was to enhance the separation efficiency of a PDMS membrane for TCE by manipulating the hydrophobicity of silicalite-1 particles using silane coupling agents APTMS, TMCS, and TMDS. Among these agents, TMDS@silicalite-1 particles exhibited the highest hydrophobicity, resulting in the MMM filled with TMDS@silicalite-1 particles demonstrating superior adsorption selectivity and PV performance for TCE. Furthermore, the impact of various operational parameters, including concentration, temperature, flow rate, and pressure, on the separation efficacy was investigated. The optimal operational parameters were determined, and an investigation was conducted to explore the separation mechanism of the modified membrane. It was found that when the temperature was set at 30 °C, the flow rate at 100 mL min<sup>-1</sup>, and the vacuum degree at 30 kPa, the TMDS@silicalite-1/PDMS MMM exhibited a separation factor of 139 and a total flux of 242 g m<sup>-2</sup> h<sup>-1</sup> for a  $3 \times 10^{-7}$  wt% TCE aqueous solution. This represents a 44% increase in separation factor and a 16% increase in TCE flux compared to the unmodified silicalite-1/PDMS membrane. Furthermore, when compared to the pure PDMS membrane, the separation factor increased by 83% and the TCE flux increased by 20%. Furthermore, the pervaporation separation of trichloroethylene (TCE) has been extensively studied, and various membranes have been previously reported.



Notably, silicalite-1@TMDS/PDMS membranes have demonstrated favorable separation factors in prior investigations. These findings provide evidence that the hydrophobic modification of inorganic fillers can considerably enhance the separation efficiency of polydimethylsiloxane (PDMS) membranes when applied to TCE aqueous solutions.

## Data availability

All relevant data used in this study can be obtained from the corresponding authors upon reasonable request.

## Author contributions

The concept and design of the study were collaborative efforts between all authors. Xiaosan Song was in charge of data collection, material preparation, and analysis. Xichen Song, Bo Liu and Zilin Yue wrote the first draft of the paper, and subsequent draughts were revised with insight from all authors. The final draft of this paper was reviewed and approved by all authors.

## Conflicts of interest

No conflict of interest was reported by the authors.

## Acknowledgements

This work was supported by the Natural Science Foundation of Gansu province (20JR10RA228).

## References

- 1 D. Si, M. Zhu, X. Sun, *et al.*, Formation process and pervaporation of high aluminum ZSM-5 zeolite membrane with fluoride-containing and organic template-free gel, *Sep. Purif. Technol.*, 2020, **257**, 117963.
- 2 Y. Peng, L. Peng, K. Chen, *et al.*, Degradation of Trichloroethylene By Photoelectrochemically Activated Persulfate, *Chemosphere*, 2020, **254**, 126796.
- 3 G. Chee, A novel whole-cell biosensor for the determination of trichloroethylene, *Sens. Actuators, B*, 2016, **237**, 836–840.
- 4 C. Courbet, A. Riviere, S. Jeannottat, *et al.*, Complementing approaches to demonstrate chlorinated solvent biodegradation in a complex pollution plume: mass balance, PCR and compound-specific stable isotope analysis, *J. Contam. Hydrol.*, 2011, **126**, 315–329.
- 5 J. Edstrom, M. Semmens, R. Hozalski, *et al.*, Stimulation of dechlorination by membrane-delivered hydrogen: small field demonstration, *Environ. Eng. Sci.*, 2015, **22**, 281–293.
- 6 J. Han, S. Lontoh and J. Semrau, Degradation of chlorinated and brominated hydrocarbons by *Methylomicrobium album* BG8, *Arch. Microbiol.*, 1999, **172**, 393–400.
- 7 Y. Kim and K. Hyun, Performance assessment on combined process of the oxidation and Biological Activated Carbon filtration for removal of Chlorinated Volatile Organic Carbons from river water, *KSCE J. Civ. Eng.*, 2017, **22**, 46–53.
- 8 C. Cheng, D. Yang, M. Bao, *et al.*, Spray-coated PDMS/PVDF composite membrane for enhanced butanol recovery by pervaporation, *J. Appl. Polym. Sci.*, 2021, **138**, 49738.
- 9 H. Azimi, A. Ebneyamini, F. Tezel, *et al.*, Separation of Organic Compounds from ABE Model Solutions via Pervaporation Using Activated Carbon/PDMS Mixed Matrix Membranes, *Membranes*, 2018, **8**, 40.
- 10 G. Shi and H. Chung, Thin film composite membranes on ceramic for pervaporation dehydration of isopropanol, *J. Membr. Sci.*, 2013, **448**, 34–43.
- 11 X. Zhan, J. Lu, T. Tan and J. Li, Mixed matrix membranes with HF acid etched ZSM-5 for ethanol/water separation: preparation and pervaporation performance, *Appl. Surf. Sci.*, 2012, **259**, 547–556.
- 12 A. Kujawska, K. Knozowaka, J. Kujawa, *et al.*, Fabrication of PDMS based membranes with improved separation efficiency in hydrophobic pervaporation, *Sep. Purif. Technol.*, 2020, **234**, 116092.
- 13 S. Li, P. Li, D. Cai, *et al.*, Boosting pervaporation performance by promoting organic permeability and simultaneously inhibiting water transport via blending PDMS with COF-300, *J. Membr. Sci.*, 2019, **579**, 141–150.
- 14 Y. Tian, C. Hu, M. An, *et al.*, Fabrication and Characterization of Carbon Nanotube Filled PDMS Hybrid Membranes for Enhanced Ethanol Recovery, *ACS Appl. Mater. Interfaces*, 2023, **15**, 12294–12304.
- 15 G. Liu, F. Xianli, W. Wei, *et al.*, Improved performance of PDMS/ceramic composite pervaporation membranes by ZSM-5 homogeneously dispersed in PDMS via a surface graft/coating approach, *Chem. Eng. J.*, 2011, **174**, 495–503.
- 16 G. Xue and B. Shi, Performance of various Si/Al ratios of ZSM-5-filled polydimethylsiloxane/polyethersulfone membrane in butanol recovery by pervaporation, *Adv. Polym. Technol.*, 2018, **37**, 3095–3105.
- 17 Z. Si, C. Liu, G. Li, *et al.*, Epoxide-based PDMS membranes with an ultrashort and controllable membrane-forming process for 1-butanol/water pervaporation, *J. Membr. Sci.*, 2020, **612**, 118472.
- 18 H. Zhou, Y. Su, X. Chen, *et al.*, Modification of silicalite-1 by vinyltrimethoxysilane (VTMS) and preparation of silicalite-1 filled polydimethylsiloxane (PDMS) hybrid pervaporation membranes, *Sep. Purif. Technol.*, 2010, **75**, 286–294.
- 19 S. Marthosa, W. Youravong, C. Kongmanklang, *et al.*, Applications and characterization of silicalite-1/polydimethylsiloxane composite membranes for the pervaporation of a model solution and fermentation broth, *Horm. Mol. Biol. Clin. Invest.*, 2019, **39**, 152–160.
- 20 N. Wang, J. Liu, J. Li, *et al.*, Tuning properties of silicalite-1 for enhanced ethanol/water pervaporation separation in its PDMS hybrid membrane, *Microporous Mesoporous Mater.*, 2015, **201**, 35–42.
- 21 K. Ramaiah, D. Satyasri, S. Sridhar, *et al.*, Removal of hazardous chlorinated VOCs from aqueous solutions using novel ZSM-5 loaded PDMS/PVDF composite membrane consisting of three hydrophobic layers, *J. Hazard. Mater.*, 2013, **261**, 362–371.



22 X. Zhan, J. Li, J. Huang, *et al.*, Pervaporation properties of PDMS membranes cured with different cross-linking reagents for ethanol concentration from aqueous solutions, *Chin. J. Polym. Sci.*, 2009, **27**, 533–542.

23 F. Xiangli, Y. Chen, W. Jin, *et al.*, Polydimethylsiloxane (PDMS)/Ceramic Composite Membrane with High Flux for Pervaporation of Ethanol–Water Mixtures, *Ind. Eng. Chem. Res.*, 2007, **46**, 2224–2230.

24 P. Guan, C. Ren, H. Shan, *et al.*, Boosting the pervaporation performance of PDMS membrane for 1-butanol by MAF-6, *Colloid Polym. Sci.*, 2021, **299**, 1459–1468.

25 S. Hu, W. Ren, D. Cai, *et al.*, A mixed matrix membrane for butanol pervaporation based on micron-sized silicalite-1 as macro-crosslinkers, *J. Membr. Sci.*, 2017, **533**, 270–278.

26 O. Larlus, V. Valtchev, J. Patarin, *et al.*, Preparation of silicalite-1/glass fiber composites by one- and two-step hydrothermal syntheses, *Microporous Mesoporous Mater.*, 2002, **56**, 175–184.

27 K. Mishra and R. Singh, Effect of APTMS modification on multiwall carbon nanotube reinforced epoxy nanocomposites, *Composites, Part B*, 2019, **162**, 425–432.

28 R. Yang, Y. Liu, K. Wang, *et al.*, Characterization of surface interaction of inorganic fillers with silane coupling agents, *J. Anal. Appl. Pyrol.*, 2003, **70**, 413–425.

29 J. Villaluenga and Y. Cohen, Numerical model of non-isothermal pervaporation in a rectangular channel, *J. Membr. Sci.*, 2005, **260**, 119–130.

30 H. Ye, X. Zhang, Z. Zhao, *et al.*, Pervaporation performance of surface-modified zeolite/PU mixed matrix membranes for separation of phenol from water, *Iran. Polym. J.*, 2017, **26**, 193–203.

31 H. Zhou, Y. Su, X. Chen, *et al.*, Separation of acetone, butanol and ethanol (ABE) from dilute aqueous solutions by silicalite-1/PDMS hybrid pervaporation membranes, *Sep. Purif. Technol.*, 2011, **79**, 375–384.

32 H. Zhou, J. Zhang, Y. Wan, *et al.*, Fabrication of high silicalite-1 content filled PDMS thin composite pervaporation membrane for the separation of ethanol from aqueous solutions, *J. Membr. Sci.*, 2017, **524**, 1–11.

33 C. Zuo, J. Hingley, X. Ding, *et al.*, Transmission of butanol isomers in pervaporation based on series resistance model, *J. Membr. Sci.*, 2021, **638**, 119702.

34 D. Sun, B. Li, Z. Xu, *et al.*, Pervaporation of ethanol/water mixture by organophilic nano-silica filled PDMS composite membranes, *Desalination*, 2013, **322**, 159–166.

35 M. Hu, Z. Wu, L. Sun, *et al.*, Improving pervaporation performance of PDMS membranes by interpenetrating polymer network for recovery of bio-butanol, *Sep. Purif. Technol.*, 2019, **228**, 115690.

36 T. Mohammadi, A. Aroujalian and A. Bakhshi, Pervaporation of dilute alcoholic mixtures using PDMS membrane, *Chem. Eng. Sci.*, 2005, **60**, 1875–1880.

37 T. Wang, T. Ansai and S. Lee, Zeolite-loaded poly(dimethylsiloxane) hybrid films for highly efficient thin-film microextraction of organic volatiles in water, *J. Chromatogr. B*, 2017, **1041**, 133–140.

38 B. Qiu, Y. Wang, S. Fan, *et al.*, Ethanol mass transfer during pervaporation with PDMS membrane based on solution-diffusion model considering concentration polarization, *Sep. Purif. Technol.*, 2019, **220**, 276–282.

39 P. Ye, Y. Zhang, H. Wu, *et al.*, Mass transfer simulation on pervaporation dehydration of ethanol through hollow fiber NaA zeolite membranes, *AIChE J.*, 2016, **62**, 2468–2478.

40 A. Kujawska, K. Knozowska, J. Kujawa, *et al.*, Influence of downstream pressure on pervaporation properties of PDMS and POMS based membranes, *Sep. Purif. Technol.*, 2016, **159**, 68–80.

41 H. Hong, L. Chen, Q. Zhang, *et al.*, The pervaporation performance and mass transfer process of PDMS membranes for acetic acid/water mixture, *E-Polym.*, 2011, **11**, 43–54.

42 H. Ahn, D. Jeong, H. Jeong, *et al.*, Pervaporation characteristics of trichlorinated organic compounds through Silicalite-1 zeolite membrane, *Desalination*, 2009, **245**, 754–762.

43 J. Jou, W. Yoshida and Y. Cohen, A novel ceramic-supported polymer membrane for pervaporation of dilute volatile organic compounds, *J. Membr. Sci.*, 1999, **162**, 269–284.

44 M. Hoshi, T. Saito, A. Higuchi, *et al.*, Separation of aqueous organic solvents through crosslinked poly(acrylate-co-acrylic acid) membranes by pervaporation, *Sen'i Gakkaishi*, 1991, **47**, 644–649.

